Numerical simulation study on the coupling of a regional climate model with a hydrological model

SUOQUAN ZHOU[1], GENGYUAN XUE[1], PENG GONG[2] & XU LIANG[3]

1 *Key Laboratory of Meteorological Calamity, Nanjing Institute of Meteorology, Nanjing 210044, Jiangsu, China*
zhousuoquan@jsmail.com.cn

2 *International Institute for Earth System Science, Nanjing University, Nanjing 210093 China*

3 *Department of Civil and Environmental Engineering, University of California, Berkeley, California 94720-1710, USA*

Abstract This paper numerically simulated the climate situation of rainstorms and surface runoff in the Yangtze basin in 1998 in China. Results show that the regional climate model (RegCM2) can successfully simulate the location and strength of the subtropical high, the Tibetan upper-air high centre and surface thermal low, the cool and warm advection to the east and west side of the Tibetan plateau, and also the confluence of north and southwesterly air flow branches over east China. On the basis of the above simulation, the model was used further to simulate precipitation, for example, the range and location of more than 600 mm rainfall, the 300 mm closed isopluvial, and the 100~500 mm precipitation area of the storm in the south of China, by coupling the general variable infiltration capability (GVIC). The study on the impact of GVIC on the regional climate simulation indicates that the GVIC runoff scheme improved the modelling of moisture convergence, increased the moisture content in the atmosphere below 700 hPa, and enhanced precipitation in the Yangtze River basin. The experiment of coupling RegCM2 with the hydrological model shows that the trend of calculated drainage is consistent with that of the observations, especially for drainage rising and fluctuation processes in June and August, respectively, in spite of some differences between their magnitudes. The simulated drainage at Yichang and Hankou, using the coupling model, are generally consistent with the observations from June to August.

Key words coupling; hydrological model; regional climate model

INTRODUCTION

Runoff, like precipitation, is influenced by climate change that influences the global hydrological cycle. It is impossible to simulate the surface hydrological balance without a dynamic climate condition. It is therefore important to study the influence of climate on the drainage of large-scale basins such as the Yangtze for the purpose of water resource management, flood prediction, etc. The surface runoff calculation is the most inaccurate part of GCM (Shi *et al.*, 2001) because we do not completely understand the interaction between the land hydrosphere and atmosphere. There are large differences between many calculation schemes concerning runoff, and it is hard to distinguish which scheme is better. Although there are many land surface process models which incorporate in detail the surface hydrological process (Ducoudre *et al.*, 1993), it is still difficult to determine how to correctly represent surface runoff in

GCM because the runoff calculation is affected by the simulation of precipitation, evaporation, and infiltration (Wigmosta *et al.*,1994).

This paper focuses on several aspects of the climate–hydrology coupling model: modifying the land surface runoff representation in RegCM2 with an inhomogeneous surface runoff algorithm which can be applied to loose and compact soil areas, and coupling a climate model with a hydrological model. Third, the important features are simulated, such as the subtropical high band and the westerly flow. Fourth, the rainstorms which took place during the heavy flood period in 1998 are simulated and compared with the observed precipitation. Finally, the discharge at two stations, Yichang and Wuhan, at the outlets of the upper and middle reaches of the Yangtze basin, is simulated in terms of the coupling hydro-climate model.

CLIMATE MODEL AND RESEARCH AREA

The general circulation model used in this paper is the RegCM2, and its dynamic framework is based on the mesoscale model MM4 (Anthes *et al.*, 1990). RegCM2, which has the function of a climate model, is coupled with the biosphere–atmosphere-transfer scheme (BATS). Chinese scientists have successfully verified the RegCM2 model, adapted some of the physical process parameterization, and determined the boundary and initial condition for the characteristics of geography and climatology in East Asia (Ding *et al.*, 1998). They have especially used the pressure gradient formulation to improve the pressure gradient calculation error resulted from applying the σ coordinate to steep topography.

The Yangtze River basin is in the centre of the research area of this paper, which covers most of China, including the Tibetan plateau, south Asia and part of west Asia. RegCM2 with 60 km × 60 km resolution totals 51 × 121 horizontal grids. The model has 10 vertical levels, i.e. 0.0, 0.15, 0.30, 0.45, 0.60, 0.75, 0.85, 0.93, 0.97, 0.99, 1.0 in the σ coordinate. The initial physical fields and the boundary condition employ the NCEP/NCAR reanalysis data (1 May–31 August 1998) with 1.875 × 1.875° resolution. The model was integrated for a total of 123 days with a 120 s time step, from 1 May to 31 August with the first 15 days as a time adjustment in May. Therefore, only the simulated results of June, July and August 1998 were analysed. A one-hour time step was for BATS, and a one-day step for the routing model. The hydrological model was provided by Dr Vivek. The flow velocity was calculated using Manning's formulation, and the digital river network was determined by the topographic relationship between RegCM2 resolution grids (Fig. 4).

SURFACE RUNOFF ALGORITHM

Numerous field studies have shown that surface runoff is mainly generated by two mechanisms, the excess infiltration runoff and the excess saturation runoff. The spatial variability of soil properties, antecedent soil moisture, topography, and rainfall will all result in different surface runoff generation. In the surface runoff parameterization scheme of BATS (used in former RegCM2), the two surface runoff generation mechanisms are not physically represented (Liang *et al.*, 2001), and also, the effect of infiltration heterogeneity in a basin on the surface runoff is not considered. The VIC model takes a series of methods to solve this problem (Liang *et al.*, 1994), but has not been coupled with climate model. This paper adopts the similar idea for improving BATS' surface runoff algorithm in RegCM2.

The generated runoff may be divided into two parts: surface runoff and underground runoff or baseflow. In the humid region, there is plenty of rainfall, a higher underground water table, and a thin layer of unsaturated soil. Although the surface layer has less water content due to evaporation, the water content under the soil layer usually reaches the field moisture capacity, and its deficit is less. Furthermore, when the soil moisture deficit isn't saturated, no runoff is generated as all the rainfall is absorbed by the soil in most parts of the humid or semihumid basin because the local plants have plentiful roots and a strong ability to penetrate water in the soil. The runoff is determined by the relationship between precipitation and soil water penetration, or by contrast soil deficit with infiltration. In other words, the runoff is determined by moisture deficit and penetration of the soil. But in other regions, there are sparse plants, compact soil and weak water penetration of the soil, the runoff is still generated when precipitation intensity is greater than the soil water penetration. The runoff is determined by rainfall intensity and soil infiltration capability. Therefore, it is necessary to develop a scheme for the general variable infiltration capability (GVIC) of the surface runoff. The scheme should be applicable not only to humid regions where the runoff is determined by precipitation and soil water penetration, but also to drought regions with compact soil where the runoff is determined by precipitation intensity and soil infiltration capability. Suppose the change in infiltration with time is represented as follows (Zhou *et al.*, 2003):

$$f(t) = f_c + (f_0 - f_c)\mathrm{e}^{-kt} \tag{1}$$

Where $f(t)$ is the infiltration capability at t time, f_c is the final infiltration capability, f_0 is the initial infiltration capability, k is a soil feature parameter, e.g. damply coefficient of soil infiltration capability with time. The value of the parameters f_0, f_c, and k, for different soil types can be found in Liang (2001). From equation (1):

$$f(t) = f_0\mathrm{e}^{-kt} + f_c(1 - \mathrm{e}^{-kt}) \tag{2}$$

Suppose:

$$f_1(t) = f_0\mathrm{e}^{-kt} \tag{3}$$

$$f_2(t) = f_c(1 - \mathrm{e}^{-kt}) \tag{4}$$

where $f_1(t)$ represents the infiltration capacity from the soil's physical characteristics at t time, and $f_2(t)$ is the penetration from the water gravity. Suppose $w_s(t)$ is the soil's water content at t time, and is generated by the soil's water penetration during 0~t time (even if there has been some water in the soil before penetration), therefore the soil's moisture can be written as follows:

$$w_s(t) = \int_0^t f_1 dt = \frac{f_0}{k}(1 - \mathrm{e}^{-kt}) \tag{5}$$

The filtration and drainage from t to $t + \Delta t$ are represented as follows, respectively:

$$\overline{f_{\Delta t}} = \frac{1}{\Delta t}\int_t^{t+\Delta t}\left[(f_0 - f_c)\mathrm{e}^{-kt} + f_c\right]\mathrm{d}t \tag{6}$$

$$\bar{j}_{\Delta t} = \frac{1}{\Delta t}\int_t^{t+\Delta t} f_c\left(1-\mathrm{e}^{-kt}\right)\mathrm{d}t \tag{7}$$

Using the field water capacity and soil moisture formulas, equations (6) and (7) are integrated as follows, respectively:

$$\bar{f}_{\Delta t} = \frac{1}{\Delta t}(W - w_s(t))\left(1-\mathrm{e}^{-k\Delta t}\right) + f_c\left[1 - \frac{W - w_s(t)}{\Delta t \cdot k \cdot W}\left(1-\mathrm{e}^{-k\Delta t}\right)\right] \tag{8}$$

$$\bar{j}_{\Delta t} = f_c - \frac{f_c}{\Delta t \cdot k}\mathrm{e}^{-kt}\left(1-\mathrm{e}^{-k\Delta t}\right) \tag{9}$$

The built formulas of soil infiltration capability describe the average infiltration capability in a basin. But there are great differences of soil water penetration for different parts of the basin. Therefore, the soil spatial infiltration heterogeneity is presented as follows. If f is the soil water infiltration capability for some place in the basin, the fraction of the area of the infiltration less than f over the total basin area is:

$$\alpha = 1 - \left(1 - \frac{f}{f_{\max}}\right)^n \tag{10}$$

This is the distribution curve of an inhomogeneous infiltration basin. $f_{\max}$ is the maximum infiltration capability in the basin. The average infiltration over a time period is $\overline{f_{\Delta t}}$ can be obtained from $\overline{f_{\Delta t}} = \int f\mathrm{d}\alpha$.

$$\overline{f_{\Delta t}} = \frac{f_{\max}}{(1+n)} \tag{11}$$

The infiltration of less than and equal to fraction α area is less than the spatial average instantaneous precipitation intensity p at t time. So, the instantaneous runoff r is equal to the precipitation p minus infiltration f. Integrate the r from 0 to p based on the infiltration distribution curve:

$$r = \int_0^p \alpha\mathrm{d}f = p - \frac{f_{\max}}{1+n}\left[1 - \left(1 - \frac{p}{f_{\max}}\right)^{1+n}\right] \tag{12}$$

Substitute equation (11) for $f_{\max}$ in (12):

$$r = p - \overline{f_{\Delta t}}\left[1 - \left(1 - \frac{p}{(1+n)\bar{f}_{\Delta t}}\right)^{1+n}\right] \tag{13}$$

Then the average runoff during Δt is:

$$R_s = P - \Delta t \cdot \overline{f_{\Delta t}} \left[1 - \left(1 - \frac{p}{(1+n)\overline{f_{\Delta t}}} \right)^{1+n} \right] \tag{14}$$

Combine equations (14) and (8) to construct the runoff algorithm.

ROUTING MODEL

The routing model is hypothetically input by surface and subsurface runoffs from the GCM hydrological process. The routing model consists of two storages or reservoirs, a surface water reservoir and a groundwater reservoir. These two reservoirs have different water travel mechanisms and time scales. The travel speed of underground water is much slower. Furthermore, we suppose that the underground reservoir feedbacks water to the surface reservoir, which is connected by river network. Based on mass conversion, the continuity equation of the model is written (Vivek, 1999):

$$\frac{\mathrm{d}s_s}{\mathrm{d}t} = Q_{si} + Q_{sr} + Q_g - Q_s \tag{15}$$

$$\frac{\mathrm{d}s_g}{\mathrm{d}t} = Q_{gr} - Q_g \tag{16}$$

Where s_s is the surface reservoir, and s_g the subsurface reservoir; Q_{si}, and Q_s are the surface water inflow from the adjacent upstream grid cell and outflow to the downstream grid cell, respectively; Q_{sr}, and Q_{gr} are the surface runoff and deep soil percolation estimations given by the land surface scheme on GCM grids; and Q_g is the groundwater outflow from the groundwater reservoir.

We assume the storage s is proportional to the outflow Q discharge: $s(t) = kQ(t)$, where k is a constant with time dimension. Q_{si} is connected by river net when the equations are applied to every grid box of GCM with river flow routing model.

$$Q_{si} = Q_{siN} + Q_{siNE} + Q_{siE} + Q_{sisE} + Q_{siS} + Q_{siSW} + Q_{siW} + Q_{siNW} \, . \tag{17}$$

The subscript *N*, *NE*, *E*, *SE*, *S*, *SW*, *W* and *NW* represent the water flow direction at a GCM grid. We numerically solve the previous partial equations at grids. The author suggests the follow second-order finite difference equation:

$$Q_s^{t+1} = Q_s^t \left(1 + \frac{\tau^2}{2k^2} - \frac{\tau}{k} \right) + \frac{\tau}{2k} Q^{t+1} + \left(\frac{\tau}{2k} - \frac{\tau^2}{2k^2} \right) Q^t \tag{18}$$

where $Q = Q_{si} + Q_{sr} + Q_g$, τ is the time step of one day. With the help of integration factor $e^{-t/kg}$ and boundary conditions, the expression of $Q_g(t)$ can be derived from equation (16).

$$Q_g(t) = e^{-t/k_g} Q_g(t-1) + (1 - e^{-t/k_g}) Q_{gr}(t) \tag{19}$$

where k_g is the groundwater delay factor in days.

SIMULATION RESULTS

Atmospheric circulation simulation

Figure 1 shows the RegCM2-simulated results and the NCEP reanalysis data in June 1998. The simulated 500 hPa height field is coincident with the NCEP data, the two-trough-one ridge pattern with a lowest height of 570 dagpm and 580 dagpm over north China. This pattern has an important influence on the rainstorm in June. The simulated stream field (Fig 1(a)) at 100 hPa indicates that south-Asia high pressure is consistent with that observed (Fig 1(b)) in position and strength. Second, the model successfully simulated the location and strength of the subtropical high, to west Tibetan plateau and the thermal low over the plateau. Southern and northern branch west-flows converge over the Yangtze River basin. The simulated stream field reflects considerably well the real field except an extra-strong simulated anticyclone over southwest to the plateau.

(a)

(b)

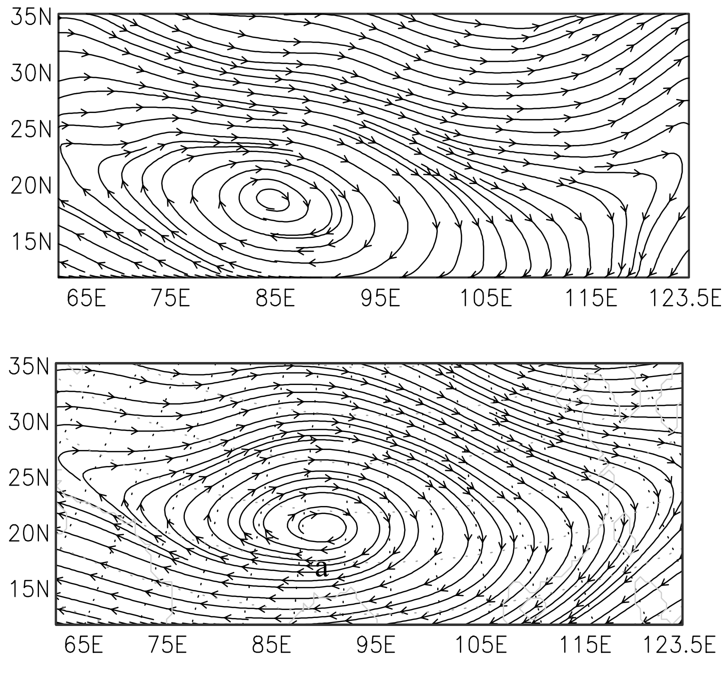

Fig. 1 The comparison of RegCM2-simulated 100hPa stream field with the NCEP reanalysis data in June 1998. (a) Simulation; (b) NCEP reanalysis data, units: dagpm.

Precipitation simulation

A lot of research indicates that the general circulation model (GCM) does not have enough ability to simulate the meso- or micro-scale precipitation processes. The simulated precipitation is usually less than the observation because the GCM's grid is usually larger than the scale of meso- or micro-scale weather systems. The GCM scarcely recognizes these weather systems that bring rainfall. Second, it's hard to obtain complete observation data of convectional clouds from growth to death. Third, it's impossible to completely describe the micro-physic process of cloud dynamics.

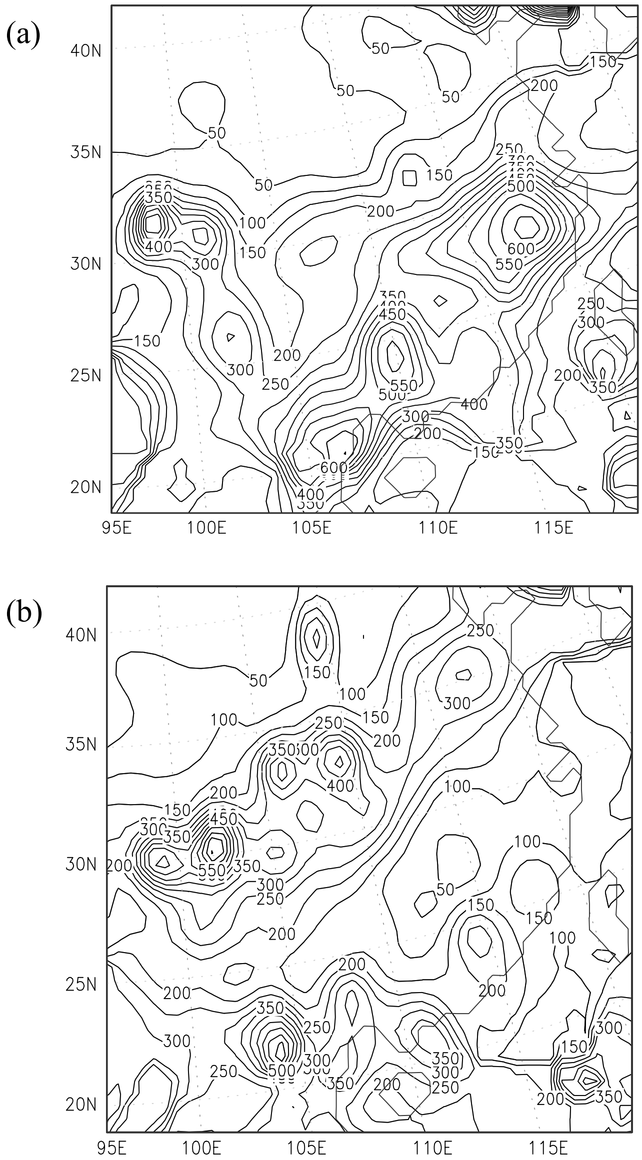

Fig. 2 The simulated precipitation in 1998: (a) June, (b) August; units, mm.

Consequentially, the parameterization of cumulus convection creates the significant error for calculating precipitation. Therefore, this paper tries to improve the precipitation simulation in terms of the moisture transportation between land surface and atmosphere, based on the suggested runoff scheme.

To focus on the Yangtze basin, this paper just draws part of the precipitation distribution. Figure 2 show the simulated rainfall for June and August by RegCM2. Most of southern China has heavy downfalls and rainstorms (Fig. 2(a)). The monthly precipitation was about 100–500 mm in the Yangtze River basin, and more than 500 mm in part of southern China, especially in the middle reaches of the Yangtze basin, resulting in flood calamities in several provinces, such as Jiangxi, Guangxi, Hunan, Zhejiang and Fujian, etc. Two maximum rain fall centres with 650 mm and 600 mm were located in the northwest of Jiangxi, southern Zhejiang, northern Fujian province roughly at 28°N 117°E and 25°N 110°E, respectively. The simulated rainfall possesses similar features to that of the observation. Although the maximum difference between simulation and observation reached 300 mm, it did not influence the veracity of the simulated precipitation distribution because the 300 mm difference only covers a small area.

The simulated precipitation in July (Figure omitted) roughly shows three maximum areas: one with 500 mm is located in the middle reaches of the Yangtze, or 30°N 107–115°E, close to the observation; the second with 600 mm in 27–30°N, 100°E, and the third in southern Guangxi province, with more precipitation and less area than the real. The July rainfall of the studied area mainly concentrates in the Yangtze basin. The rain band (Fig. 2(b)) of August stretches from the southwest to the northeast, or from the southeast to the plateau in the Shandong peninsula with a 400 mm area in northern Jiangsu and southern Shandong; 450 mm area in the middle reaches of the Yangtze, a small 600 mm area around 22°N 103°E, or the southeast to the plateau. These rainfall concentration areas consist of a rain band accordant with the observed precipitation. On the whole the RegCM2 almost simulated correctly the precipitation and its distribution in the summer of 1998, although there are some differences between the measured data and the simulation.

EFFECT OF RUNOFF SCHEME ON REGIONAL CLIMATE SIMULATION

The surface runoff indirectly influences the mass and energy exchange between terrain and atmosphere, thereby the regional climate. Figure 3(a) is the simulated 500 hPa temperature difference field using GVIC and BATS's runoff schemes. It indicates that the temperature field is influenced systematically by different runoff schemes. The simulated temperature using GVIC decreases by 0.5–1.0 K at 850 hPa, and temperature increases by 0.5–2.0 at 700 hPa, 500 hPa. This phenomenon probably reveals that the low atmosphere is cooled down by evaporation, and the upper atmosphere is heated by extra-moisture condensation.

(a) (b)

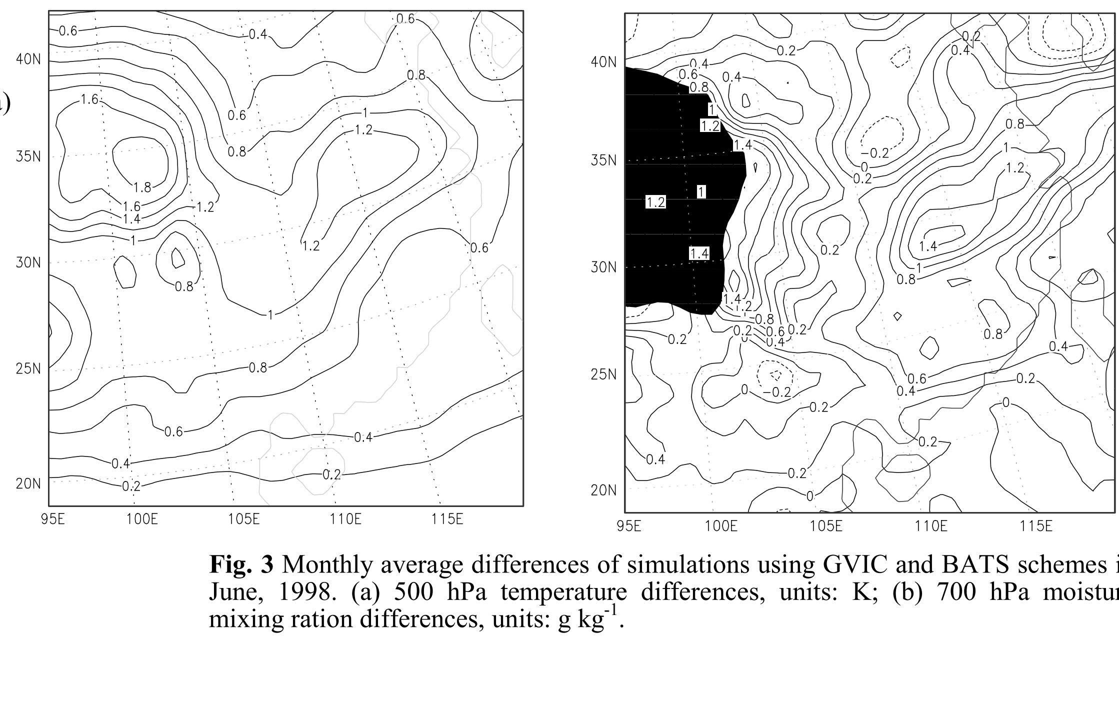

Fig. 3 Monthly average differences of simulations using GVIC and BATS schemes in June, 1998. (a) 500 hPa temperature differences, units: K; (b) 700 hPa moisture mixing ration differences, units: g kg^{-1}.

The wind difference field (figure omitted) demonstrates the GVIC's contribution to the airflow convergence that plays an important role in the rainstorm in June 1998. The wind difference shows the 700 hPa cyclonic shear in the middle reaches of the Yangtze River. There is a strong south wind difference in the south side of the shear, which steers the moist airflow to the Yangtze basin. The convergence of 700 hPa difference flow indicates that the GVIC facilitates the form of the rainstorm circulation, which transfers the moisture from the low levels to the upper levels, and thus increases simulated rainfall in the Yangtze basin. This might possibly mean that evaporation is enhanced in the low level, and condensation is increased in the upper level.

The moisture mixing ratio differences of about 1.5 g kg^{-1}–1.8 g kg^{-1} (Fig. 3(b)) at 700 hPa reflect the contribution of GVIC to atmospheric moisture, and the moisture exchange between air and terrain. There are mixing ratio positive differences at 700 hPa, and the maximum positive difference is consistent with the rainstorm location in the Yangtze basin, demonstrating that the GVIC improves the precipitation simulation by increasing the moisture in atmosphere below 700 hPa.

HYDRO-CLIMATE COUPLING SIMULATION

The simulated climate element fields at each time step, such as precipitation, temperature, vapour pressure etc. from RegCM2 are simultaneously input into the land surface process model BATS using the GVIC runoff scheme, and the surface runoff is obtained from integrating the GVIC scheme hourly. Based on the Yangtze River water system, the digital river network (Fig. 4) is obtained on the RegCM2 60 km × 60 km resolution grids. The river channels pass through the centre of every cell that the water flow direction is determined as one of the eight directions by the river water system. The output water from the cell flows into the downstream cell. Based on the assumption of the relationship between travel distance and velocity, water in all grid cell flows have same time delay coefficient. The travel distance is determined according to the shortest distance principle.

Figure 5 compares the daily steam flow simulated by the coupling climate model with the observed hydrograph for the Yangtze River at Yichang and Hangkou stations. It is shown that the simulated drainage curve rises monotonously as the real curve, from 12 June to 4 July when five great rainstorms took place in the Yangtze basin. In

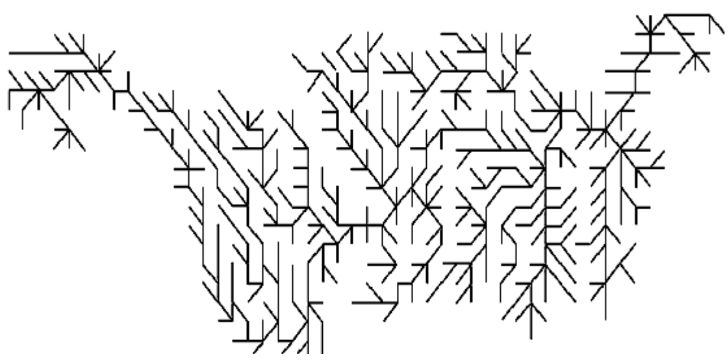

Fig. 4 The digital river network of the Yangtze River on RegCM2 grids (60 km × 60 km).

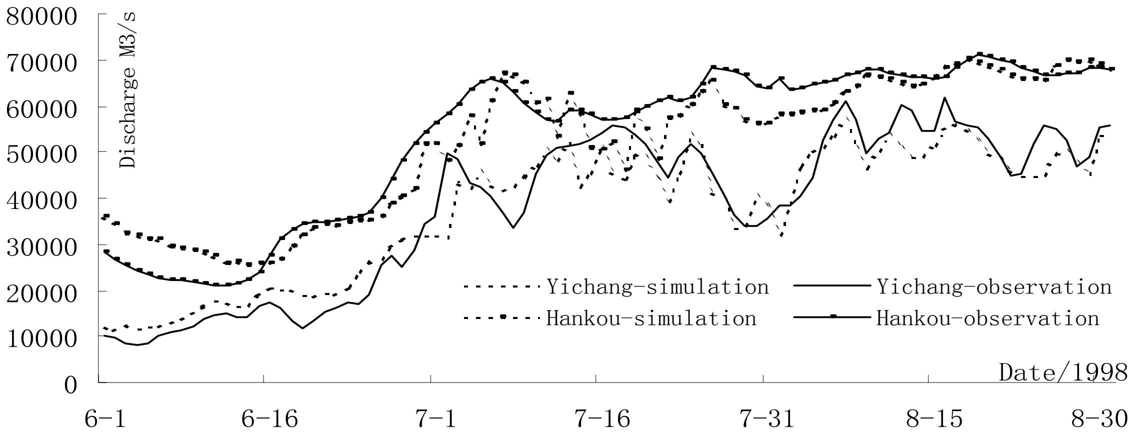

Fig. 5 Discharges at Yichang and Hankou simulated using the coupling model (unit: $m^3 s^{-1}$).

July, the simulated discharge is much less than the real value due to the distinguished simulation error of precipitation resulted from much convection action of the mouth in atmosphere. Because the coupling model isn't able to represent the intense convection weather system whose spatial scale is less than model grid. The modelling value isn't completely consistent with the real value. But the modelling curve in August oscillates at a high discharge level; and afterwards the simulated discharge decreases gradually. Modelling curves characterize the observation well.

CONCLUSION

This paper verified firstly the modelling results using the NCEP reanalysis data in the rainstorm period (May to August) 1998. The verification indicates that RegCM2 simulated successfully major climate features of June general circulation pattern and June and August precipitation.

The GVIC surface runoff scheme correctly simulates the June and August rainfall simulation of RegCM2. The area and position of the simulated monthly 300 mm rainfall contour are very close to the observation, simulated by the RegCM2 with the BATS scheme. The impact analysis of GVIC on simulated height, temperature, wind and stream fields demonstrate that the GVIC enhances the convergent ascent of model atmosphere moisture at the 700 hPa level, and thus increases evaporation in the lower and condensation in the upper atmosphere.

This paper couples the RegCM2 with a hydrological model to simulate the drainage at Yichang and Hankou, and the simulated discharge is approximately consistent with the observation from June to August in 1998. The simulated increasing and smooth periods of discharge are rather coincident with those of the observations, reflecting that the GVIC scheme is probably more reasonable than the BATS runoff scheme. However, there are still some temporal and spatial differences between simulated and observed precipitation in July in the Yangtze basin, which may indicate that there must be other factors influencing the precipitation simulation.

Acknowledgements Funding for this work was provided by the Ministry of Science and Technology and National Natural Science Foundation of China (Project Number 2001CB309404, 40128001/D05, 49375248).

REFERENCES

Anthes, R. A., Kuo, Y. H. & Gyakum, J. R. (1990) Numerical simulations of a case of explosive marine cyclogenesis. *Mon. Wea. Rev.* **111**, 1174–1188.

Ding, Y., Zhang, J. & Zhao, Z. (1998) The study of modeling experiment of a improving land surface Part II: The coupling modeling experiment of land surface model with regional climate model, *Acta Meteorologica Sinica* **56**(4), 385–399.

Ducoudre, N. I., Laval, K. & Perrier, A. (1993) SECHIBA, a new set of parameterization of the hydrologic exchange at the land-atmosphere interface within the LMD atmospheric general circulation model. *J. Climat*, **6**, 248–269.

Liang, X. & Xie, Z. (2001) A new surface runoff parameterization with subgrid-scale soil heterogeneity for land surface models. *Adv. Water Resour.* **24**, 1173–1193.

Liang, X., Lettenmair, D. P., Wood, E. F. & Burges, S. J. (1994) A simple hydrologically based model of land surface water and energy fluxes for general circulation models. *J. Geophy Res*. **99**(D7), 14415–14428.

Shi, X. (2001) The review of study on land surface process model, *J. Appl. Meteorol. of China* **12**(1), 102–112.

Vivek, K. A. (1999) A river flow routing scheme for general circulation models. *J. Geophys. Res.* **104**(D12), 14347–14357.

Wigmosta, M. S., Lance, W. V. & Lettenmaier, D. P. (1994) A distributed hydrology-vegetation model for complex terrain. *Water Resour. Res.* **30**(6), 1665–1679.

Zhou, S., Dai, K., Chen, T. & Tu, Q. (2003a) The improvement and verification of land surface process model (BATS). *Acta Meteorolohica Sinica* **61**(3), 275–290.